Available online at www.sciencedirect.com
SCIENCE DIRECT®
ELSEVIER
Composite Structures 74 (2006) 399–405
COMPOSITE STRUCTURES
www.elsevier.com/locate/compstruct

Damage detection of surface cracks in composite laminates using modal analysis and strain energy method

Huiwen Hu [a,*], Bor-Tsuen Wang [b], Cheng-Hsin Lee [a], Jing-Shiang Su [a]

[a] Department of Vehicle Engineering, National Pingtung University of Science and Technology, Neipu, Pingtung 91201, Taiwan
[b] Department of Mechanical Engineering, National Pingtung University of Science and Technology, Neipu, Pingtung 91201, Taiwan

Available online 8 June 2005

Abstract

This paper presents an approach to detect surface cracks in various composite laminates. Carbon/epoxy composite AS4/PEEK was used to fabricate laminated plates, $[0]_{16}$, $[90]_{16}$, $[(0/90)_4]_S$ and $[\pm45/0/90]_{2S}$. Surface crack damage was created on one side of the plate using a laser cutting machine. Modal analysis was performed to obtain the mode shapes from both experimental and finite element analysis results. The mode shapes were then used to calculate strain energy using the differential quadrature method (DQM). Consequently, the strain energies of laminated plates before and after damaged were used to define a damage index which successfully identified the surface crack location.

Keywords: Composite laminates; Damage detection; Modal analysis; Strain energy; DQM

1. Introduction

The application of modal analysis to detect damage in composite materials has been increasingly adopted due to its flexibility of measurement and relatively low cost. The basic idea is to use information on modal parameters, such as natural frequencies, mode shapes and damping ratios, to access the structural damage.

Cawley and Adams [1,2] simply used the frequency shifts for different modes to detect the damage in composite structures. Tracy and Pardoen [3] found that the natural frequencies of a composite beam were affected by the size and damage location. Shen and Grady [4] found that local delamination does not have a noticeable effect on global mode shape of vibration of composite beams, but delamination does cause irregularity of mode shapes. Pandey et al. [5] also showed that the irregular of mode shape is significant for relatively large damage. However, Saravanos and Hopkins [6] indicated that small delaminations may not be detectable by monitoring the global characteristics of a composite beam. Zou et al. [7] provided a thorough review on vibration-based techniques and indicated that the above methods were unable to detect very small damage and required large data storage capacity for comparisons.

Cornwell et al. [8] utilized the measured mode shapes to calculate the strain energy of a steel plate. In his approach, fractional strain energy of the plate before and after damaged was used to define a damage index, which was used to locate the damage in the steel plate. The method only requires the mode shapes of the structure before and after damage. Nevertheless, the challenge of the approach lies in the accuracy of measured modes. A large amount of data points are required for further analysis to locate the damage. To solve this problem, Hu et al. [9] adapted the DQM to obtain a solution of strain energy of a composite plate. It was reported that the original DQM was first used in structural mechanics problems by Bert et al. [10]. This method is able to rapidly compute accurate solutions of partial differential

* Corresponding author. Tel.: +886 8 7703202x7452; fax: +886 8 7740398.
E-mail address: huiwen@mail.npust.edu.tw (H. Hu).

0263-8223/$ - see front matter © 2005 Elsevier Ltd. All rights reserved.
doi:10.1016/j.compstruct.2005.04.020

equations by using only a few grid points in the respective solution domains [11].

The objective of this paper is to apply modal analysis and the strain energy method to the damage detection of a surface crack in various composite laminated plates. Both experimental modal analysis (EMA) and finite element analysis (FEA) were performed to obtain the mode shapes of the laminated plates. The mode shapes were then used to calculate the strain energy using DQM. Consequently, a damage index was established to locate the surface crack using the fractional strain energy of laminated plates before and after damaged.

2. Modal analysis

2.1. Experiment

Carbon/epoxy composite AS4/PEEK was used in this study. Laminated plates with unidirectional fiber orientation laminates, i.e., $[0]_{16}$ and $[90]_{16}$; cross-ply laminate, i.e., $[(0/90)_4]_S$; and quasi-isotropic laminate, i.e., $[\pm 45/0/90]_{2S}$ were fabricated by stacking up the prepreg and then curing in a hot-press machine. After curing, the panel was cut to a $209 \times 126 \times 2.4\ \mathrm{mm}^3$ laminate using a diamond saw. A 25 mm long and 1 mm deep surface crack was created at one side near the center by using a laser cutting machine.

Modal testing was conducted on the laminated plates as shown in Fig. 1. Test plate was marked with 13×13 parallel grid points, and vertically hung by two cotton strings to simulate completely free boundary conditions. The test plate was excited by an impact hammer with a force transducer throughout all grid points. The dynamic responses were measured by an accelerometer fixed at the corner of the test plate. A Siglab, Model 20–40, was used to record the frequency response functions (FRFs) between the measured acceleration and impact force. ME'Scope, a software for general purpose curve fitting, was used to extract modal parameters, i.e., natural frequencies, damping ratios and mode shapes, from the FRFs. In this study, measured mode shapes of the test plate are the only demands for further analysis.

2.2. Finite element analysis

A FE model was established to simulate the laminated plate. ANSYS, a FEA commercial code, was used in this study. Eight-node linear solid element (SOLID46) was adopted for the modeling. This element type provides a layered version allow up to 250 different material layers. To simulate a surface crack, the nodes at location of surface crack were replaced by separated nodes as shown in Fig. 2. Hu et al. [12] found that the mass effect of the accelerometer significantly affects the dynamic responses and should not be neglected in finite element model. Thus, a mass element (MASS21) with 0.002 kg was assigned to the finite element model [12].

Mechanical properties of composite AS4/PEEK ($E_1 = 140.3$ GPa, $E_2 = E_3 = 9.4$ GPa, $G_{12} = G_{13} = 5.4$ GPa, $\nu_{12} = \nu_{13} = 0.253$) were entered into ANSYS. These data were obtained from the tensile tests of the material. Since the effect of out-of-plane shear modulus G_{23} and Poisson's ratio ν_{23} are not evident in thin plate, the values of G_{23} and ν_{23} were assumed to be the same as G_{12} and ν_{12}. Material density of the plates is measured to be about 1520 kg/m^3.

Normal mode analysis was performed to obtain the natural frequencies and the associated mode shapes of the plates, up to 2 kHz. A convergence study was performed to obtain a $40 \times 30 \times 8$ mesh model, which is sufficient to solve the normal mode problem. However, to simulate the experiment, an analysis using with mesh model $13 \times 13 \times 8$ was also performed and used in comparison with experimental results.

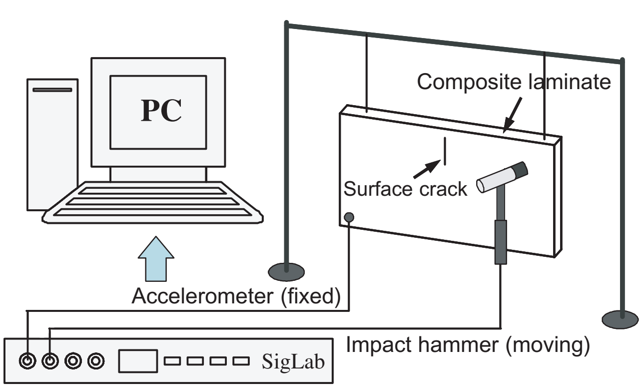

Fig. 1. Experimental set-up.

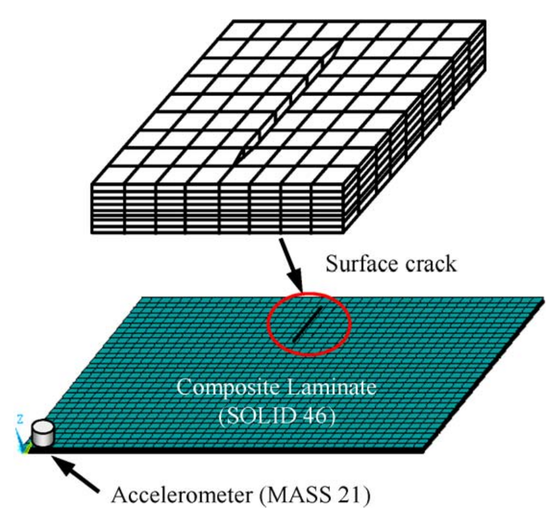

Fig. 2. Finite element model for damaged laminate.

3. Strain energy method and damage index

The fractional strain energy of laminated plate before and after damaged are used to define the damage index in this approach. Fig. 3 shows the grid point arrangement of a test plate. The plate was subdivided into $N_x \times N_y$ sub-region and denoted the location of each point by (x_i, y_j). During elastic deformation, the strain energy of laminated plate is given by

$$U = \frac{1}{2}\int_0^b \int_0^a \left[D_{11}\left(\frac{\partial^2 w}{\partial x^2}\right)^2 + D_{22}\left(\frac{\partial^2 w}{\partial y^2}\right)^2 + 2D_{12}\frac{\partial^2 w}{\partial x^2}\frac{\partial^2 w}{\partial y^2} + 4\left(D_{16}\frac{\partial^2 w}{\partial x^2} + D_{26}\frac{\partial^2 w}{\partial y^2}\right) \times \frac{\partial^2 w}{\partial x \partial y} + 4D_{66}\left(\frac{\partial^2 w}{\partial x \partial y}\right)^2 \right] \mathrm{d}x\,\mathrm{d}y \tag{1}$$

where w is the transverse displacement of the plate, D_{ij} are the bending stiffnesses of the plate. For a particular mode shape ϕ_k, the energy associated with the mode shape is expressed as

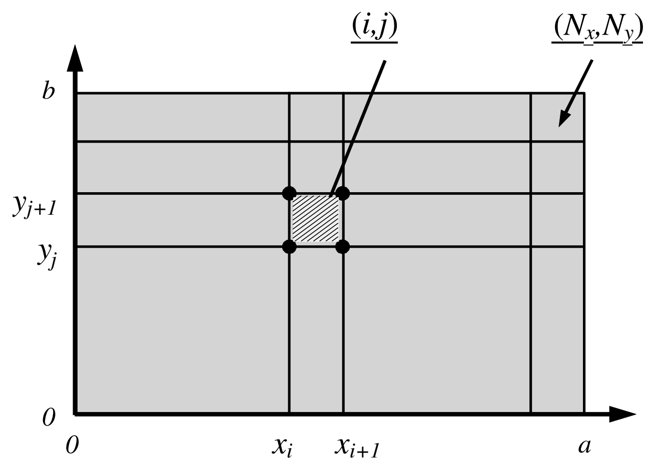

Fig. 3. Grid points arrangement.

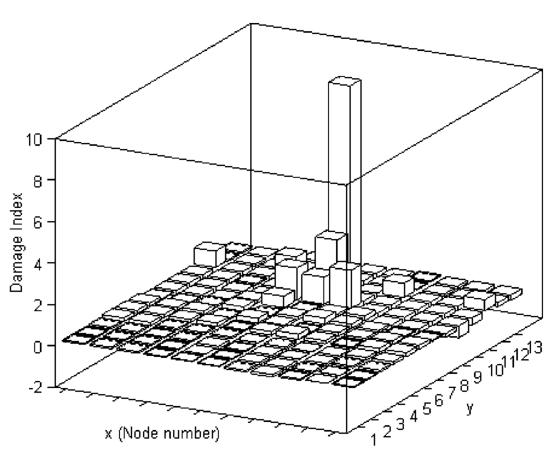

Fig. 4. Damage index for laminated plate $[0]_{16}$ (FEA).

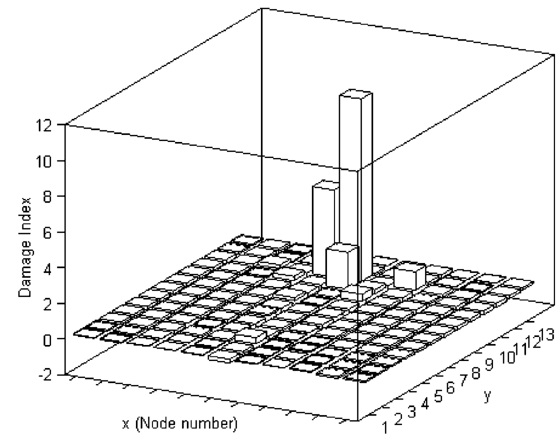

Fig. 5. Damage index for laminated plate $[90]_{16}$ (FEA).

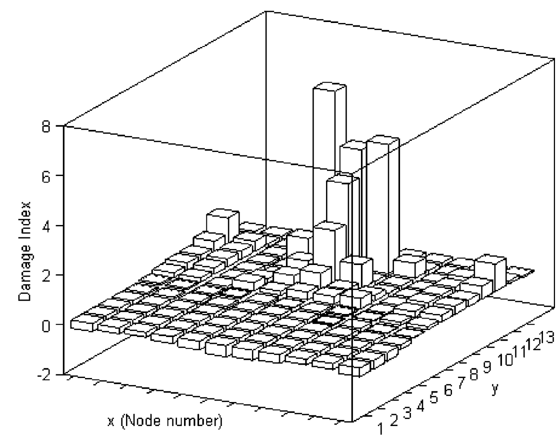

Fig. 6. Damage index for laminated plate $[(0/90)_4]_S$ (FEA).

$$U_k = \frac{1}{2}\int_0^b \int_0^a \left[D_{11}\left(\frac{\partial^2 \phi_k}{\partial x^2}\right)^2 + D_{22}\left(\frac{\partial^2 \phi_k}{\partial y^2}\right)^2 + 2D_{12}\frac{\partial^2 \phi_k}{\partial x^2}\frac{\partial^2 \phi_k}{\partial y^2} + 4\left(D_{16}\frac{\partial^2 \phi_k}{\partial x^2} + D_{26}\frac{\partial^2 \phi_k}{\partial y^2}\right) \times \frac{\partial^2 \phi_k}{\partial x \partial y} + 4D_{66}\left(\frac{\partial^2 \phi_k}{\partial x \partial y}\right)^2 \right] \mathrm{d}x\,\mathrm{d}y \tag{2}$$

Cornwell et al. [8] suggested that if the damage is located at a single sub-region then change in the bending stiffness of the sub-region can be used to locate the damage. Thus, the energy associated with sub-region (i,j) for the kth mode is given by

$$U_{k,ij} = \frac{1}{2}\int_{y_j}^{y_{j+1}} \int_{x_i}^{x_{i+1}} \left[D_{11}\left(\frac{\partial^2 \phi_k}{\partial x^2}\right)^2 + D_{22}\left(\frac{\partial^2 \phi_k}{\partial y^2}\right)^2 + 2D_{12}\frac{\partial^2 \phi_k}{\partial x^2}\frac{\partial^2 \phi_k}{\partial y^2} + 4\left(D_{16}\frac{\partial^2 \phi_k}{\partial x^2} + D_{26}\frac{\partial^2 \phi_k}{\partial y^2}\right) \times \frac{\partial^2 \phi_k}{\partial x \partial y} + 4D_{66}\left(\frac{\partial^2 \phi_k}{\partial x \partial y}\right)^2 \right] \mathrm{d}x\,\mathrm{d}y \tag{3}$$

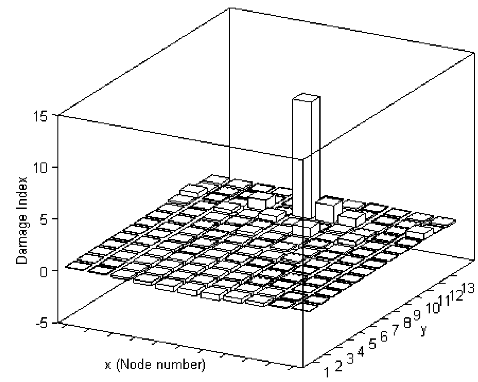

Fig. 7. Damage index for laminated plate $[\pm 45/0/90]_{2S}$ (FEA).

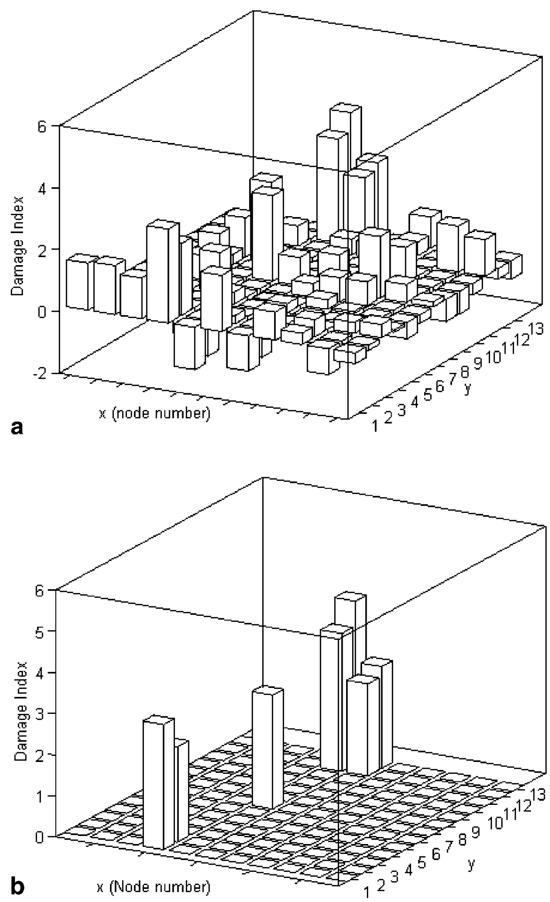

Fig. 8. Damage index for laminated plate $[0]_{16}$ (EMA): (a) before truncation and (b) after truncation.

A fractional energy is defined as

$$F_{k,ij} = \frac{U_{k,ij}}{U_k} \tag{4}$$

The summation of all fractional energies should be equal to unity, i.e.,

$$\sum_{j=1}^{N_y} \sum_{i=1}^{N_x} F_{k,ij} = 1 \tag{5}$$

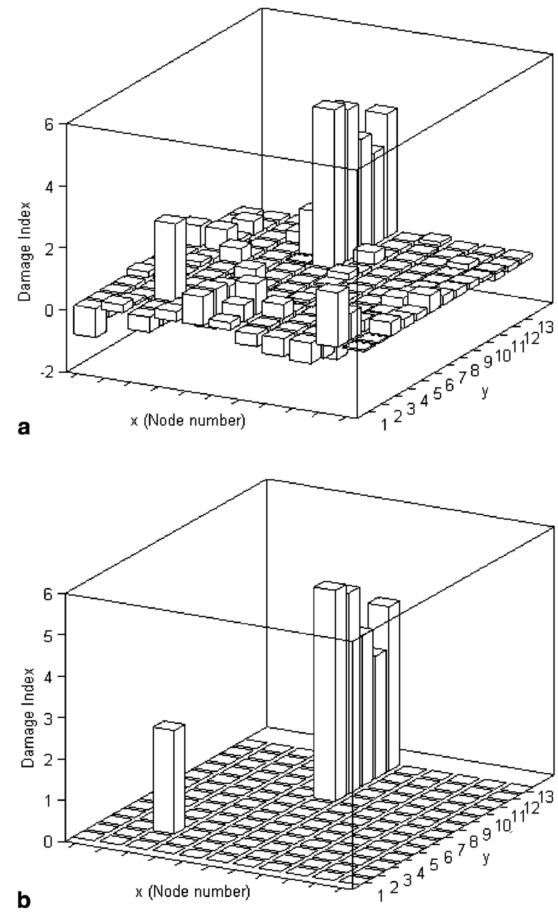

Fig. 9. Damage index for laminated plate $[90]_{16}$ (EMA): (a) before truncation and (b) after truncation.

Similarly, U_k^* and $U_{k,ij}^*$ represent the total strain energy and the sub-regional strain energy of the kth mode shape ϕ_k^* for damaged plate. Thus, a fractional energy of damage plate is given by

$$F_{k,ij}^* = \frac{U_{k,ij}^*}{U_k^*} \tag{6}$$

Certainly, we have

$$\sum_{j=1}^{N_y} \sum_{i=1}^{N_x} F_{k,ij}^* = 1 \tag{7}$$

Considering all measured modes m, damage index in sub-region (i,j) is defined as

$$\beta_{ij} = \frac{\sum_{k=1}^{m} F_{k,ij}^*}{\sum_{k=1}^{m} F_{k,ij}} \tag{8}$$

A normalized damage index is given by

$$Z_{ij} = \frac{\beta_{ij} - \overline{\beta}_{ij}}{\sigma_{ij}} \tag{9}$$

where $\overline{\beta}_{ij}$ and σ_{ij} represent the mean and standard deviation of the damage indices, respectively. The

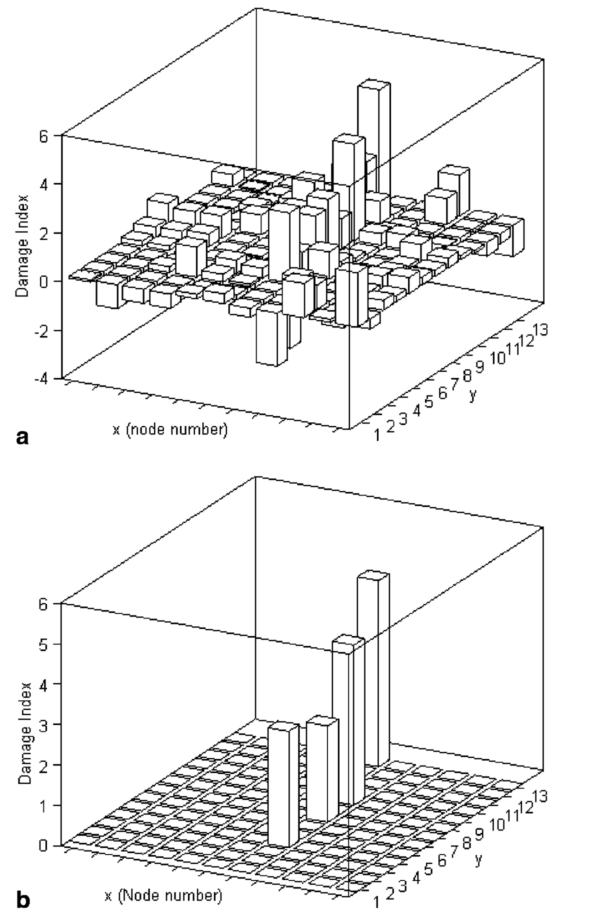

Fig. 10. Damage index for laminated plate $[(0/90)_4]_S$ (EMA): (a) before truncation and (b) after truncation.

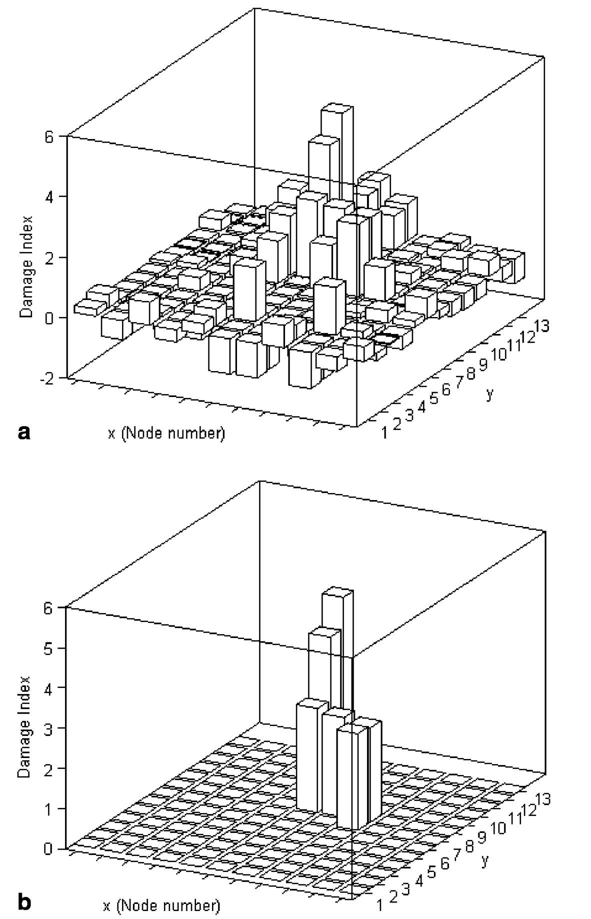

Fig. 11. Damage index for laminated plate $[\pm 45/0/90]_{2S}$ (first EMA): (a) before truncation and (b) after truncation.

calculations of partial differential terms in strain energy formula are complicated. An alternative numerical method DQM was therefore introduced to solve the problem.

4. Differential quadrature method

The basic idea of DQM is to approximate the partial derivatives of a function $f(x_i, y_j)$ with respect to a spatial variable at any discrete point as the weighted linear sum of the function values at all the discrete points chosen in the solution domain of spatial variable. This can be expressed mathematically as

$$f_x^{(n)}(x_i, y_j) = \sum_{r=1}^{N_x} C_{ir}^{(n)} f(x_r, y_j) \tag{10}$$

$$f_y^{(m)}(x_i, y_j) = \sum_{s=1}^{N_y} \overline{C}_{js}^{(m)} f(x_i, y_s) \tag{11}$$

$$f_{xy}^{(n+m)}(x_i, y_j) = \sum_{r=1}^{N_x} C_{ir}^{(n)} \sum_{s=1}^{N_y} \overline{C}_{js}^{(m)} f(x_r, y_s) \tag{12}$$

where $i = 1, 2, \ldots, N_x$ and $j = 1, 2, \ldots, N_y$ are the grid points in the solution domain having $N_x \times N_y$ discrete number of points. $C_{ir}^{(n)}$ and $\overline{C}_{js}^{(m)}$ are the weighting coefficients associated with the nth order and the mth order partial derivatives of $f(x_i, y_j)$ with respect to x and y at the discrete point (x_i, y_j) and $n = 1, 2, \ldots, N_x - 1$, $m = 1, 2, \ldots, N_y - 1$. The weighting coefficients can be obtained using the following recurrence formulae:

$$C_{ir}^{(n)} = n\left(C_{ii}^{(n-1)} C_{ir}^{(1)} - \frac{C_{ir}^{(n-1)}}{x_i - x_r}\right) \tag{13}$$

$$\overline{C}_{js}^{(m)} = n\left(\overline{C}_{jj}^{(m-1)} \overline{C}_{js}^{(1)} - \frac{\overline{C}_{js}^{(n-1)}}{y_j - y_s}\right) \tag{14}$$

where i, $r = 1, 2, \ldots, N_x$ but $r \neq i$; $n = 2, 3, \ldots, N_x - 1$; also $j, s = 1, 2, \ldots, N_y$ but $s \neq j$; $m = 2, 3, \ldots, N_y - 1$. The weighting coefficients when $r = i$ and $s = j$ are given as

$$C_{ii}^{(n)} = -\sum_{r=1, r\neq i}^{N_x} C_{ir}^{(n)} \quad i = 1, 2, \ldots, N_x \quad \text{and} \quad n = 1, 2, \ldots, N_x - 1 \tag{15}$$

$$\overline{C}_{jj}^{(m)} = -\sum_{s=1, s\neq j}^{N_y} \overline{C}_{js}^{(m)} \quad j = 1,2,\ldots,N_y \quad \text{and}$$
$$m = 1,2,\ldots,N_y - 1 \tag{16}$$

$$C_{ir}^{(1)} = \frac{M^{(1)}(x_i)}{(x_i - x_r)M^{(1)}(x_r)} \quad i,r = 1,2,\ldots,N_x \quad \text{but} \quad r \neq i \tag{17}$$

$$\overline{C}_{js}^{(1)} = \frac{P^{(1)}(y_j)}{(y_j - y_s)P^{(1)}(y_s)} \quad j,s = 1,2,\ldots,N_y \quad \text{but} \quad j \neq s \tag{18}$$

For Eqs. (17) and (18), $M^{(1)}$ and $P^{(1)}$ are denoted by the following expressions:

$$M^{(1)}(x_i) = \prod_{r=1, r\neq i}^{N_x} (x_i - x_r) \tag{19}$$

$$P^{(1)}(y_j) = \prod_{s=1, s\neq j}^{N_y} (y_j - y_s) \tag{20}$$

The above equations are applied to compute the strain energy once the kth mode shape $\phi_{k,ij} = f_k(x_i, y_j)$ is obtained from either EMA or FEA.

5. Results and discussions

In FEA results, the first six mode shapes were used to calculate the strain energy and to define the damage index of the laminated plates. Figs. 4 and 5 show the damage indices of surface crack in laminated plates $[0]_{16}$ and $[90]_{16}$. The peak values simply reveal the location of surface crack in laminated plates. Encouraging results are also shown in Figs. 6 and 7. Damage indices successfully locate the surface crack in laminated plates $[(0/90)_4]_S$ and $[\pm 45/0/90]_{2S}$, respectively. Excellent results of damage indices were obtained from a fine mesh FE model. Nevertheless, the outcomes obtained from a $13 \times 13 \times 8$ mesh model are good enough to be validated by experimental results.

In EMA results, using the first six modes, damage index for laminated plates $[0]_{16}$ is shown in Fig. 8(a). Peak values occur around the surface crack location, but some also emerge at other undamaged areas. Irregularities of mode shapes caused by poor measurement in some grid points may induce these pseudomorphs. Cornwell et al. [8] suggested that damage indices with values greater than two are associated with potential damage locations. Thus, this study tried to truncate the values of damage indices smaller than two. The damage indices of surface crack become clearer as shown in Fig. 8(b). Damage indices of surface cracks in laminated plates $[90]_{16}$, $[(0/90)_4]_S$ and $[\pm 45/0/90]_{2S}$ are shown in Figs. 9–11, respectively. The peak values simply reveal the surface crack location. Similarly, clearer damage indices are obtained after truncation. In practical applications, structural health can be monitored throughout its service life. The summation of damage indices monitored at different times may magnify the signal of damage. Fig. 12 shows another result of damage index for quasi-isotropic laminated plate $[\pm 45/0/90]_{2S}$. Adding the second result to the first in Fig. 11, damage indices of surface crack become more pronounced and identifiable as shown in Fig. 13.

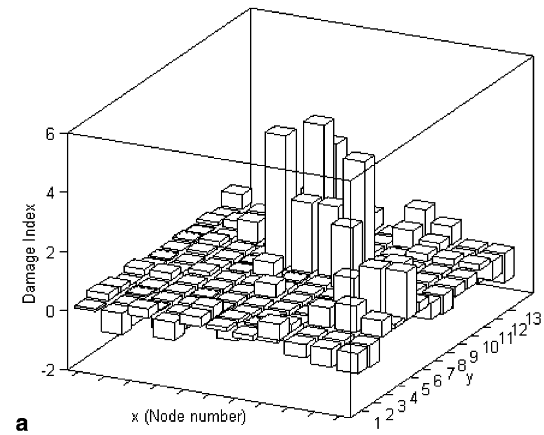

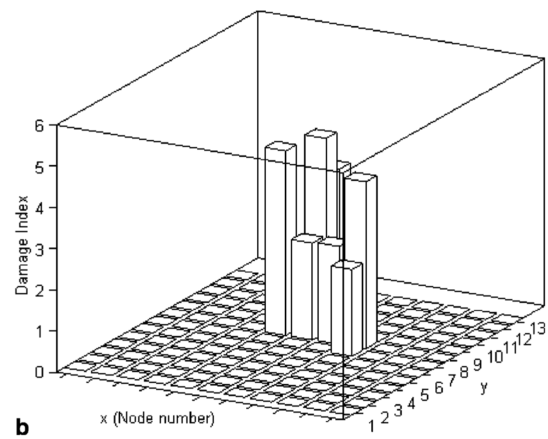

Fig. 12. Damage index for laminate plate $[\pm 45/0/90]_{2S}$ (second EMA): (a) before truncation and (b) after truncation.

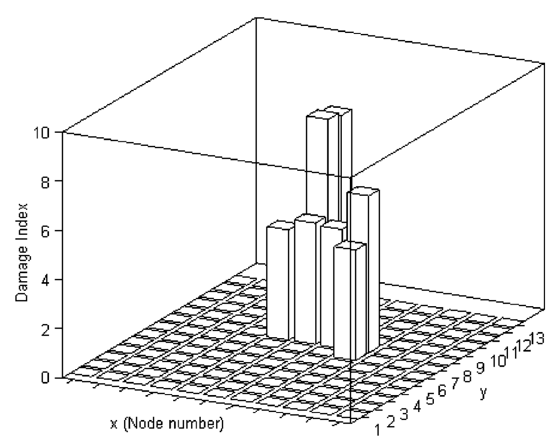

Fig. 13. Damage index for laminated plate $[\pm 45/0/90]_{2S}$ (first + second EMA).

6. Conclusions

A damage index using modal analysis and strain energy methods was developed to detect a surface crack in composite laminates. Experimental results show that surface crack locations in various composite laminates are successfully identified by the damage indices. A reliable finite element model was also developed and validated for further analysis. This method only requires a few mode shapes of a laminated plate before and after damaged. Since the number of measured points is limited, DQM provides us an accurate and rapid approach to obtain strain energy by using only a few grid points in the test plate. Further research work may lie in the sensitivity studies of measurement by using different sensors and the application of this method to various types of damage.

Acknowledgement

The authors would like to acknowledge the support of Taiwan National Science Council through grant No. NSC-92-2212-E-020-010.

References

[1] Cawley P, Adams RD. A vibration technique for non-destructive testing of fiber composite structures. J Compos Mater 1979;13:161–75.
[2] Cawley P, Adams RD. The location of defects in structure from measurements of natural frequencies. J Strain Anal 1979;14:49–57.
[3] Tracy JJ, Pardoen GC. Effect of delamination on the natural frequencies of composite laminates. J Compos Mater 1989;23:1200–15.
[4] Shen MHH, Grady JE. Free vibration of delaminated beams. AIAA J 1992;30:1361–70.
[5] Pandey AK, Biswas M, Samman MM. Damage detection form changes in curvature mode shapes. J Sound Vib 1991;145:321–32.
[6] Saravanos DA, Hopkins DA. Effects of delaminations on the damped dynamic characteristic of composite laminates: analysis and experiments. J Sound Vib 1996;195:977–93.
[7] Zou Y, Tong L, Steven GP. Vibration-based model-dependent damage (delamination) identification and health monitoring for composite structures. A review. J Sound Vib 2000;2:357–78.
[8] Cornwell PJ, Dobeling SW, Farrar CR. Application of the strain energy damage detection method to plate-like structures. In: Proceedings of the international model analysis conference—IMAC; 1997. p. 1312–18.
[9] Hu H, Wang BT, Su JS. Application of modal analysis to damage detection in composite laminates. In: The 7th ASME biennial conference on engineering system design and analysis; 2004, no. 58296.
[10] Bert CW, Jang SK, Striz AG. Two new approximate methods for analyzing free vibration of structural components. AIAA J 1988;26:612–8.
[11] Bellman RE, Kashef BG, Casti J. Differential quadrature: a technique for the rapid solution of nonlinear partial differential equation. J Comput Phys 1972;10:40–52.
[12] Hu H, Wang BT, Lee CH, Su JS. Free vibration analysis of damaged composite laminates. In: The 21th Taiwan national conference on mechanical Engineering; 2004, no. C0300804.